Papanatsiou, M., Petersen, J., Henderson, L., Wang, Y., Christie, J.M. and Blatt, M.R. (2019) Optogenetic manipulation of stomatal kinetics improves carbon assimilation, water use, and growth. Science, 363(6434), pp. 1456-1459.

There may be differences between this version and the published version. You are advised to consult the publisher's version if you wish to cite from it.

http://eprints.gla.ac.uk/180897/

Deposited on: 8 April 2019

Enlighten – Research publications by members of the University of Glasgow
http://eprints.gla.ac.uk

Optogenetic manipulation of stomatal kinetics improves carbon assimilation and water use efficiency

One sentence summary Speeding stomatal responses of the model plant Arabidopsis with the addition of an engineered ion channel enhances photosynthesis while reducing the physiological costs of fluctuating light.

Papanatsiou, M.[1], Petersen, J.[1,2], Henderson, L.[1], Wang, Y.[1,3], Christie, J.M.[1,4], and Blatt, M.R.[1,3,4]

[1]Laboratory of Plant Physiology and Biophysics and the Plant Science Group, Institute of Molecular, Cell and Systems Biology, University of Glasgow, University Avenue, G12 8QQ, UK

[2]Institute of General Botany and Plant Physiology, Friedrich Schiller University, Am Planetarium 1, 07743 Jena, Germany

[3]Institute of Crop Science, College of Agriculture and Biotechnology, Zijingang Campus, Zhejiang University, Hangzhou, China

[4]Joint senior authors; please direct correspondence to michael.blatt@glasgow.ac.uk

Abstract

Stomata serve dual and often conflicting roles, facilitating CO_2 influx into the plant leaf for photosynthesis and restricting water efflux via transpiration. Thus, strategies for reducing transpiration without a cost for photosynthesis must circumvent this inherent coupling of CO_2 and water vapor diffusion. We expressed the synthetic, light-gated K^+ channel, BLINK1, in guard cells surrounding stomatal pores to enhance the solute fluxes that drive stomatal aperture. BLINK1 introduced a K^+ conductance and accelerated both stomatal opening in the light and

closing following irradiation. Integrated over the growth period, BLINK1 drove a 2.2-fold increase in biomass in fluctuating light without cost in water use by the plant. Thus, we demonstrate the potential of enhancing stomatal kinetics to improve water use efficiency without penalty in carbon fixation.

Main text

Stomata are pores in the leaf epidermis that form between pairs of guard cells. They allow CO_2 uptake for photosynthetic carbon assimilation at the expense of water loss via transpiration, thereby influencing global carbon and hydrological cycles (*1*, *2*). Stomatal aperture is controlled by guard cell turgidity which responds to changes in atmospheric CO_2 concentration, light, atmospheric relative humidity, and abscisic acid (*5*-*8*), thereby regulating plant water use. Efforts to improve plant water use efficiency have focused on reducing stomatal density, despite its implicit penalty in carbon assimilation (*3*, *4*). Approaches that circumvent the carbon:water trade-off pose greater challenges but also much promise. In particular, accelerating the kinetics of stomatal opening and closing could be used to promote carbon assimilation under high light intensities, while maintaining plant water status when carbon demand is low (*3*, *4*). Here we have used the synthetic, Blue Light-INduced K^+ channel 1 (BLINK1) as a tool for modulating guard cell K^+ conductance and accelerating changes in stomatal aperture with light. We demonstrate that a strategy of enhancing stomatal kinetics is sufficient to promote photosynthetic carbon assimilation and water use efficiency (WUE). Thus, BLINK1, and related optogenetic tools offer ways to explore plant growth and its relationship to WUE without a cost in CO_2 availability for photosynthesis.

Opening and closing of stomata is driven by ion transport across the guard cell plasma membrane which, together with the metabolism of organic solutes, promotes water flux and changes in guard cell volume and turgor. Blue light (BL) triggers stomatal opening, among

other responses, enhancing photosynthesis through the action of the phototropin receptor kinases phot1 and phot2 that lead to activation of guard-cell H^+-ATPases, in turn promoting K^+ uptake (*5*, *9*, *10*). We therefore explored whether stomatal opening could be augmented by tissue-specific expression of the optogenetic tool BLINK1.

BLINK1 is a synthetic, blue light-gated K^+ channel, constructed by fusing the LOV2-Jα photo-switch from *Avena sativa* phot1 to the small viral K^+ channel Kcv; when expressed in human embryonic kidney cell cultures, it introduces a K^+ conductance that is independent of voltage and activated by BL with half-maximal saturation near 40 μmol m^{-2} s^{-1} (*11*). To confirm that BLINK1 also functions in plants, initially we expressed BLINK1 transiently in tobacco and in Arabidopsis root epidermal cells (*12*). Immunoblots showed BLINK1 formed tetramers expected of the functional K^+ channel (Fig. S1). On treatments with 100 μmol m^{-2} s^{-1} BL, membrane voltages of root epidermal cells bathed in 30 mM K^+ showed mean displacements of 15 mV amplitude toward the predicted K^+ equilibrium voltage, as expected on activating a K^+ conductance (Fig. S2). From the voltage kinetics, we concluded that the conductance was fully activated within 2 min +BL and decayed over 8-10 min on transfer to dark.

To analyze BLINK1 function in guard cells, we used a strong guard cell-specific promoter (*13*) to express the synthetic channel in wild-type (wt) Arabidopsis (wt-BLINK) and, as a background control, in the *phot1phot2* (*p1p2*) (*14*) double mutant (*p1p2*-BLINK). Transcript analysis showed that *BLINK1* was expressed at comparable levels in two independent *p1p2*-BLINK and wt-BLINK transgenic lines (Fig. 1b and Fig. S3). We measured the plasma membrane conductance using two-electrode recording methods (*15*) on intact guard cells of *p1p2*-BLINK and wt-BLINK transgenic lines, comparing conductances with each to the corresponding *p1p2* and wt backgrounds. Close to the free-running voltage, the membrane conductance of Arabidopsis guard cells is normally small, making it difficult to resolve, by voltage clamp, the conductance changes that would suffice to enhance K^+ flux and accelerate

79 stomatal movements (Material & Methods). We therefore used a current clamp to drive 0.5-s
80 steps of ±100 pA at intervals across the plasma membrane of dark-adapted guard cells isolated
81 in epidermal peels. We monitored the resulting changes in voltage before, during, and after
82 illuminating with 100 μmol m^{-2} s^{-1} BL (Fig. 1b, inset) and calculated the change in membrane
83 conductance ±BL (ΔG) from Ohm's Law (Fig. 1b). Photoactivation of BLINK1 led to
84 increased conductance in guard cells of *p1p2*-BLINK and of wt-BLINK plants compared to
85 the *p1p2* mutant and wt controls, respectively, with a 1.6-fold increase in ΔG of wt-BLINK
86 plants (Fig. 1b). Thus, we concluded that BLINK1 introduces a BL-dependent K^+ conductance
87 in the plasma membrane of guard cells.
88 To examine whether BLINK1 photoactivation can alter stomatal opening, we recorded
89 stomatal apertures in epidermal peels exposed to either red light (RL) or BL fluence rates of
90 100 μmol m^{-2} s^{-1} for 2 hours. BLINK1 restored BL-induced stomatal opening in the *p1p2*
91 double-mutant background (Fig. 2a) and enhanced the steady-state apertures of wt-BLINK
92 plants on average by 17% compared to the wt background in BL (Fig. 2b). Similar apertures
93 were observed for all plants under RL, indicating that the effects were BL-specific and
94 demonstrating the potential for BLINK1 to augment stomatal opening *in vivo*. To assess
95 stomatal kinetics with BLINK1, we used gas exchange and analysed the stomatal conductances
96 of intact plants ±BL after dark and RL adaptation (Fig. 2c-f and Fig. S4). Compared to the wt,
97 stomatal conductance was elevated in the *p1p2* background in the dark, consistent with
98 previous observations (*16*). Against this background, significant increases in stomatal
99 conductance were recovered in each case in the *p1p2*-BLINK transgenics with 100 μmol m^{-2}
100 s^{-1} BL, whereas *p1p2* double-mutant plants were unresponsive to BL (Fig. 2c). BLINK1
101 expression in the wt background led to 22-29% enhancements in stomatal conductance in BL
102 (Fig. 2d), despite a small reduction in stomatal size in one line (Fig. S7). Mean stomatal
103 opening and closing halftimes were accelerated by approximately 40% compared to the wt
104 controls (Fig. 2e).

Pre-adapting plants to 200 μmol m^{-2} s^{-1} RL ensures a substantial background of photosynthetic energy input to reduce CO_2 concentration within the leaf and reflects a more natural background for analyzing stomatal movements. As expected, no significant differences in steady-state transpiration, and hence in stomatal conductances, were observed between the wt-BLINK and wt plants; in this background, adding 100 μmol m^{-2} s^{-1} BL elevated stomatal conductance in all plants (Table S1). However, wt-BLINK plants showed accelerated changes in stomatal conductance, with 60-70% reductions in stomatal opening and closing halftimes compared to wt plants (Figs. 2f and S4). BLINK1 activity is independent of voltage and declined over 8-10 min (Figs. 1, S2 and (*11*)), so the accelerated kinetics for stomatal closing is consistent with BLINK1-promoted K^+ efflux as well as influx subject to the electrochemical potential for K^+ across the guard cell membrane.

One measure of plant productivity is water use efficiency, defined either as the amount of dry mass produced per unit water transpired (WUE) or as the ratio of the instantaneous rates of carbon assimilation over transpiration (WUEi). Both measures are affected by light through the combined influence on carbon demand and associated transpiration (*17*). We therefore examined the BLINK1 transgenic lines grown under diel cycles with daylight periods of constant white light, either at a low fluence rate (LWL) of 75 μmol m^{-2} s^{-1} or at a high fluence rate (HWL) of 190 μmol m^{-2} s^{-1}. We calculated WUEi over these periods and determined WUE as the ratio of accumulated dry biomass to water used over the 49-day growth period. Under the LWL and HWL treatment, growth of wt-BLINK and *p1p2*-BLINK transgenic plants showed no significant differences in biomass accumulation, rosette area expansion, or water use when compared with that of the corresponding wt and *p1p2* backgrounds (Fig. S5, S6 and Table S1).

In the natural environment light fluctuates, for example as clouds pass over. Photosynthesis generally tracks light energy input, but stomata are slower to respond. The slower stomatal kinetics limits gas exchange and can lead to suboptimal assimilation when

fluence rate rises and to transpiration without corresponding assimilation when the fluence rate drops quickly (*3*, *17*). Because BLINK1 accelerated stomatal movements (Fig. 2) we predicted that, when integrated over periods of fluctuating light, BLINK1 could benefit carbon assimilation and water use. We therefore examined the BLINK1 transgenic lines grown with daylight periods of fluctuating WL (FWL) to give a total photon flux over the daylight period intermediate to the two continuous light regimes. We stepped fluence rates ranging between 10 and 150 μmol m^{-2} s^{-1} at 60-min intervals, which is close to the time normally required for stomatal opening (Fig. 2) and therefore would maximize any advantages afforded by BLINK. No significant difference was evident in WUEi (Fig. 3b). However, rosette area and fresh weight increased in wt-BLINK transgenic plants compared to the wt control (Fig. 3e and Tables S2 and S3), and we found a 2.2-fold increase in total dry biomass of plants grown under both water-replete and water-deficit conditions which, for similar rates of steady-state transpiration, translates to an equivalent and highly significant improvement in WUE in the wt-BLINK plants (Fig. 3f). We observed a modest increase in total protein content and decrease in starch in water-replete-grown plants, and a highly significant increase in total starch in water-deficit-grown plants (Fig. S8) The wt-BLINK plants showed significant decreases in fresh/dry weight ratios under both conditions (Tables 2 and 3). Much of this biomass is likely therefore to be accounted for by changes in cell wall material. We confirmed that this increased biomass was not the consequence of alterations in photosynthesis *per se* (*18*): CO_2 assimilation under saturating light (1000 μmol m^{-2} s^{-1}) was unaffected in wt-BLINK plants across the physiological range of internal CO_2 concentrations (Fig. 3c), and the Ci/Ca ratios determined at 70, 200 and 600 μmol m^{-2} s^{-1} of white light were similar to wt plants in each case (Fig. 3d). Thus, we conclude that guard-cell expression of BLINK1 and the accelerated stomatal kinetics afforded by the synthetic channel are responsible for enhancing carbon assimilation without a cost in water use.

Optogenetics has revolutionised the study of the mammalian nervous circuitry (*11*, *19*). Because of the high output gain possible in regulating neuronal membrane voltage, the ion fluxes introduced by rhodopsin-based pumps and channels have proven sufficient to control rapid nervous signal transmission (*20*, *21*). Introducing BLINK1 into guard cells now demonstrates the application potential for optogenetics to manipulate net ion flux in plant cells which, over periods of many minutes, can directly alter cell volume and osmotically-related physiology. As many plant 'movements', growth, and morphogenic phenomena rely on solute flux to drive turgor and cell expansion, optogenetics offers new strategies with which to study and control these processes.

Our findings also have implications for strategies to improve crop WUE and enhance net photosynthetic carbon assimilation. Much research to date has focused on enhancing WUE by reducing stomatal densities, an approach that suppresses the overall conductance of the leaf but also reduces CO_2 availability for photosynthesis and can slow plant growth (*3*, *22-25*). Manipulating the native populations of ion channels and pumps has been shown to affect stomatal conductance and photosynthesis, but generally at the expense of carbon assimilation or of WUE (*15*, *26-28*). Indeed, a systems analysis of stomatal physiology shows that manipulating transporter populations alone is unlikely to improve stomatal performance and that alterations targeting the control of transport, including channel gating, are more likely to be effective (*28*). Our findings now demonstrate the efficacy of introducing new controls on guard cell membrane transport: incorporating BLINK1 adds a light-driven conductance that accelerates stomatal opening and closing to match the temporal demands for guard cell ion flux. Our findings highlight the gains that might be achieved by enhancing stomatal kinetics under changing light environments. Furthermore, we demonstrate that stomatal speed (*3*) can improve WUE without a cost in carbon assimilation. Enhancing guard cell ion flux with available light is an effective strategy to match stomatal movements with the often conflicting

demands of safeguarding water use, at the same time gaining in photosynthetic assimilation during vegetative growth.

References

1. A. M. Hetherington, F. I. Woodward, The role of stomata in sensing and driving environmental change. *Nature*. **424**, 901–908 (2003).
2. S. Jasechko *et al.*, Terrestrial water fluxes dominated by transpiration. *Nature*. **496**, 347–350 (2013).
3. T. Lawson, M. R. Blatt, Stomatal Size, Speed, and Responsiveness Impact on Photosynthesis and Water Use Efficiency. *Plant Physiology*. **164**, 1556–1570 (2014).
4. L. McAusland *et al.*, Effects of kinetics of light-induced stomatal responses on photosynthesis and water-use efficiency. *New Phytologist*. **211**, 1209–1220 (2016).
5. M. Jezek, M. R. Blatt, The Membrane Transport System of the Guard Cell and Its Integration for Stomatal Dynamics. *Plant Physiology*. **174**, 487–519 (2017).
6. S. M. Assmann, T. Jegla, Guard cell sensory systems: recent insights on stomatal responses to light, abscisic acid, and CO2. *Current Opinion in Plant Biology*. **33**, 157–167 (2016).
7. C. B. Engineer *et al.*, CO2 Sensing and CO2 Regulation of Stomatal Conductance: Advances and Open Questions. *Trends in Plant Science*. **21**, 16–30 (2016).
8. Y. Wang *et al.*, Unexpected Connections between Humidity and Ion Transport Discovered Using a Model to Bridge Guard Cell-to-Leaf Scales. *Plant Cell*. **29**, 2921–2939 (2017).
9. J. M. Christie, Phototropin Blue-Light Receptors. *Annu. Rev. Plant Biol.* **58**, 21–45 (2007).

206 10. A. Takemiya, S. Inoue, M. Doi, T. Kinoshita, K. Shimazaki, Phototropins promote plant
207 growth in response to blue light in low light environments. *The Plant Cell*. **17**, 1120–
208 1127 (2005).
209 11. C. Cosentino *et al.*, Optogenetics. Engineering of a light-gated potassium channel.
210 *Science*. **348**, 707–710 (2015).
211 12. Z. Chen, C. Grefen, N. Donald, A. Hills, M. R. Blatt, A bicistronic, Ubiquitin-10
212 promoter-based vector cassette for transient transformation and functional analysis of
213 membrane transport demonstrates the utility of quantitative voltage clamp studies on
214 intact Arabidopsis root epidermis. *Plant Cell Environ*. **34**, 554–564 (2011).
215 13. E. Cominelli *et al.*, A guard-cell-specific MYB transcription factor regulates stomatal
216 movements and plant drought tolerance. *Current Biology*. **15**, 1196–1200 (2005).
217 14. J. M. Christie, J. Gawthorne, G. Young, N. J. Fraser, A. J. Roe, LOV to BLUF:
218 Flavoprotein Contributions to the Optogenetic Toolkit. *Mol Plant*. **5**, 533–544 (2012).
219 15. Y. Wang *et al.*, Systems dynamic modeling of a guard cell Cl- channel mutant uncovers
220 an emergent homeostatic network regulating stomatal transpiration. *Plant Physiology.*
221 **160**, 1956–1967 (2012).
222 16. T. Kinoshita *et al.*, Phot1 and phot2 mediate blue light regulation of stomatal opening.
223 *Nature*. **414**, 656–660 (2001).
224 17. R. W. Pearcy, Sunflecks and photosynthesis in plant canopies. *Annu. Rev. Plant Biol.*
225 (1990).
226 18. T. D. Sharkey, C. J. Bernacchi, G. D. Farquhar, E. L. Singsaas, Fitting photosynthetic
227 carbon dioxide response curves for C(3) leaves. *Plant Cell Environ*. **30**, 1035–1040
228 (2007).
229 19. J. Mattis *et al.*, Principles for applying optogenetic tools derived from direct comparative
230 analysis of microbial opsins. *Nat Meth*. **9**, 159–172 (2012).

20. E. G. Govorunova, O. A. Sineshchekov, R. Janz, X. Liu, J. L. Spudich, Natural light-gated anion channels: A family of microbial rhodopsins for advanced optogenetics. *Science*. **349**, 647–650 (2015).

21. V. Gradinaru *et al.*, Molecular and cellular approaches for diversifying and extending optogenetics. *Cell*. **141**, 154–165 (2010).

22. T. Doheny-Adams, L. Hunt, P. J. Franks, D. J. Beerling, J. E. Gray, Genetic manipulation of stomatal density influences stomatal size, plant growth and tolerance to restricted water supply across a growth carbon dioxide gradient. *Philosophical Transactions of the Royal Society B: Biological Sciences*. **367**, 547–555 (2012).

23. J. Masle, S. R. Gilmore, G. D. Farquhar, The *ERECTA* gene regulates plant transpiration efficiency in *Arabidopsis*. *Nature*. **436**, 866–870 (2005).

24. J. Hughes *et al.*, Reducing stomatal density in barley improves drought tolerance without impacting on yield. *Plant Physiology*, pp.01844.2016 (2017).

25. Y. Tanaka, T. Nose, Y. Jikumaru, Y. Kamiya, ABA inhibits entry into stomatal-lineage development in Arabidopsis leaves. *The Plant Journal*. **74**, 448–457 (2013).

26. J. Negi *et al.*, CO2 regulator SLAC1 and its homologues are essential for anion homeostasis in plant cells. *Nature*. **452**, 483–486 (2008).

27. K. Kusumi, S. Hirotsuka, T. Kumamaru, K. Iba, Increased leaf photosynthesis caused by elevated stomatal conductance in a rice mutant deficient in SLAC1, a guard cell anion channel protein. *Journal of Experimental Botany*. **63**, 5635–5644 (2012).

28. Y. Wang, A. Hills, M. R. Blatt, Systems analysis of guard cell membrane transport for enhanced stomatal dynamics and water use efficiency. *Plant Physiology*. **164**, 1593–1599 (2014).

29. S. Bordage, S. Sullivan, J. Laird, A. J. Millar, & H. G. Nimmo, Organ specificity in the plant circadian system is explained by different light inputs to the shoot and root clocks. *New Phytologist*. **212**, 136–149 (2016).

30. J. M. Christie, T. E. Swartz, R. A. Bogomolni, & W. R. Briggs, Phototropin LOV domains exhibit distinct roles in regulating photoreceptor function. *Plant Journal.* **32,** 205–219 (2002).

31. E. Cominelli, *et al.* DOF-binding sites additively contribute to guard cell-specificity of AtMYB60 promoter. *BMC Plant Biology*. **11,** 162 (2011).

32. A. M. Davis, A. Hall, A. J. Millar, C. Darrah, & S. J. Davis, Protocol: Streamlined sub-protocols for floral-dip transformation and selection of transformants in Arabidopsis thaliana. *Plant Methods*. **5,** 3–7 (2009).

33. S. Sullivan, J. Petersen, L. Blackwood, M. Papanatsiou, & J. M. Christie, Functional characterization of Ostreococcus tauri phototropin. *New Phytologist.* **209,** 612–623 (2015).

34. C. Grefen, & M. R. Blatt, A 2in1 cloning system enables ratiometric bimolecular fluorescence complementation (rBiFC). *BioTechniques.* **53,** 311–314 (2012).

35. E. Kaiserli, S. Sullivan, M. A. Jones, K. A. Feeney, & J. M. Christie, Domain swapping to assess the mechanistic basis of Arabidopsis phototropin 1 receptor kinase activation and endocytosis by blue light. *The Plant Cell*. **21,** 3226–3244 (2009).

36. G. Romani, *et al.* A virus-encoded potassium ion channel is a structural protein in the chlorovirus Paramecium bursaria chlorella virus 1 virion. *Journal of General Virology*. **94,** 2549–2556 (2013).

37. M. Papanatsiou, A. Amtmann, & M. R. Blatt, Stomatal Spacing Safeguards Stomatal Dynamics by Facilitating Guard Cell Ion Transport Independent of the Epidermal Solute Reservoir. *Plant Physiology*. **172,** 254–263 (2016).

38. M. R. Blatt & C. L. Slayman, KCl leakage from microelectrodes and its impact on the membrane parameters of a nonexcitable cell. *Journal of Membrane Biology*. **72,** 223–234 (1983).

39. M. R. Blatt, Electrical characteristics of stomatal guard cells: The ionic basis of the membrane potential and the consequence of potassium chlorides leakage from microelectrodes. *Planta*. **170,** 272–287 (1987).

40. Y. Wang & M. R. Blatt, Anion channel sensitivity to cytosolic organic acids implicates a central role for oxaloacetate in integrating ion flux with metabolism in stomatal guard cells. *Biochemical Journal*. **439,** 161–170 (2011).

Acknowledgements We are grateful to Prof. Anna Moroni for providing the anti-Kcv antibody and to her and Prof. Tracy Lawson for their comments on the manuscript.

Funding This research was supported by the Biotechnology and Biological Sciences Research Council (grants BB/L019025/1, BB/L001276/1 and BB/M001601/1 to M.R.B., and BB/M002128/1 and BB/R001499/1 to J.M.C.).

Author Contributions M.P., J.P., J.M.C. and M.R.B. designed the study; J.P. generated constructs, screened and isolated the Arabidopsis transgenic lines and performed transient expression in tobacco; Y.W. carried out transient transformations and measurements in roots; M.P. performed the physiological and eletrophysiological characterization of transgenic lines with assistance from L.H.; M.P., J.M.C. and M.R.B. analyzed the data; M.P, J.M.C. and M.R.B wrote the manuscript. All authors discussed and commented on the manuscript.

Competing interests The authors declare no competing interests.

Correspondence and requests for materials should be addressed to M.R. Blatt (michael.blatt@glasgow.ac.uk).

List of Supplementary materials

Material and Methods

Fig S1-S8

Table S1-S3

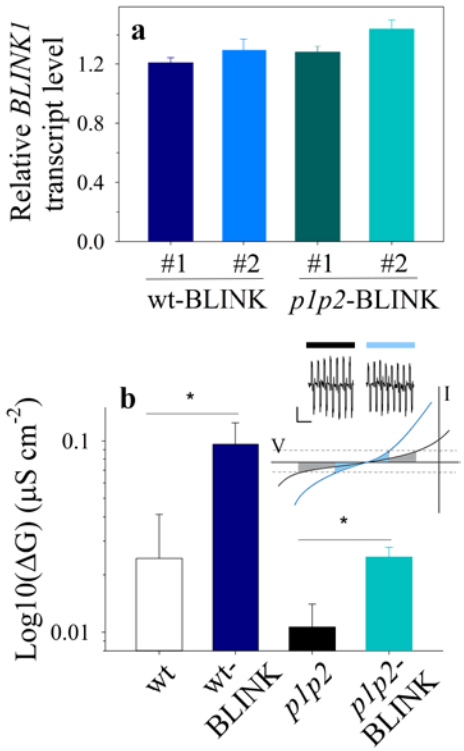

316

317

318 **Figure 1. BLINK1 expression *in planta* facilitates K^+ fluxes across guard cell plasma**
319 **membrane. (a)** qRT-PCR analysis of relative *BLINK1* transcript levels normalised to reference
320 gene *ISU*(*29*) (n=4). **(b)** Change in membrane conductance ±BL as means ±SE (n=4).
321 Significance determined by student's t-test: wt/wt-BLINK, P=0.036; *p1p2/p1p2*-BLINK,
322 P=0.022. *Inset (above)*: Voltage deflections on current clamp with ±100 pA in 0.5-s steps.
323 Scale bar: 10 mV, vertical;, 5 s, horizontal. *Inset (below)*: Schematic to show the consequence
324 for fixed-amplitude current steps on membrane voltage before (black) and during (blue) BL to
325 introduce an increase in conductance. Grey and blue shading indicates the range of voltage
326 deflections. Dotted lines indicate current clamp amplitude.

327

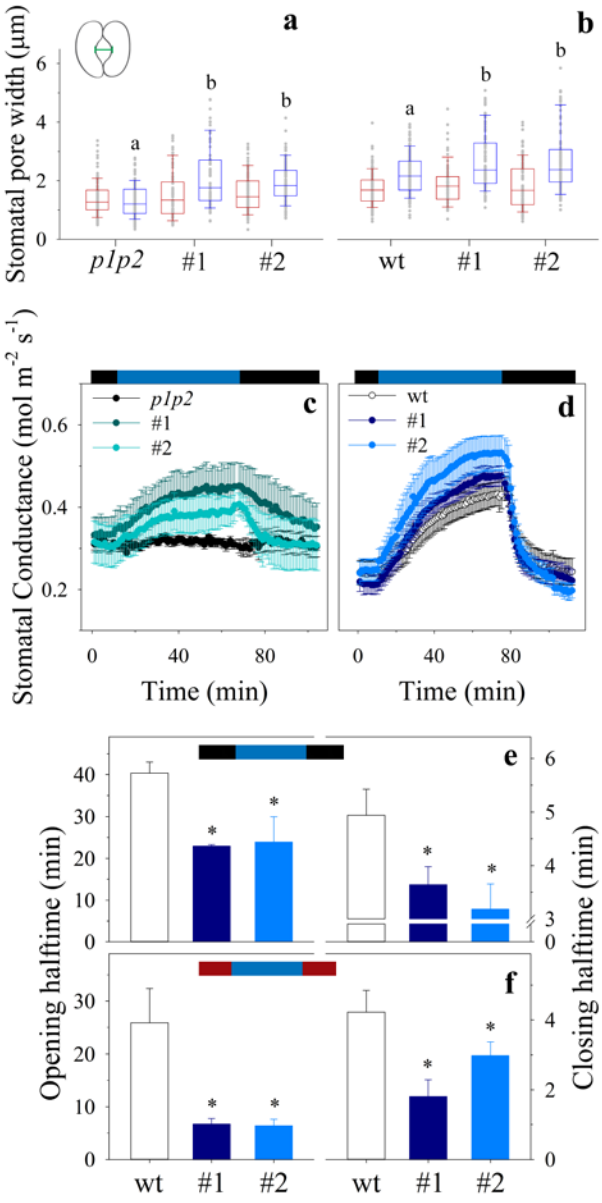

Figure 2. BLINK1 photoactivation promotes stomatal opening and accelerates stomatal kinetics. (a,b) BLINK1 restoration of BL-induced stomatal opening in the *p1p2* double mutant **(a)** and enhanced BL-induced stomatal opening in the wt background **(b)**. Data are means ±SE (n>100). Lettering indicates statistically significant differences from the wild-type and *p1p2* backgrounds, as determined by Kruskal-Wallis ANOVA on Ranks (P<0.05). *Inset*: Schematic of stomatal pore width for measurement. **(c,d)** Stomatal conductances measured from *p1p2* and *p1p2*-BLINK plants **(c)** and from wild-type and wt-BLINK plants **(d)** before, during and after 100 µmol m^{-2} s^{-1} BL treatments. **(e,f)** Halftimes for stomatal opening and closing of wt and wt-BLINK plants with steps from dark **(e)** and against a background of 100 µmol m^{-2} s^{-1} RL **(f)**

were estimated by non-linear least-squares fitting of data following light transitions to a simple exponential function. Data are means ±SE (n=5) from wt (white) and the two wt-BLINK lines (dark and light blue) in each case. Asterisks indicate statistically significant differences, as determined by student's t-test ($P<0.05$).

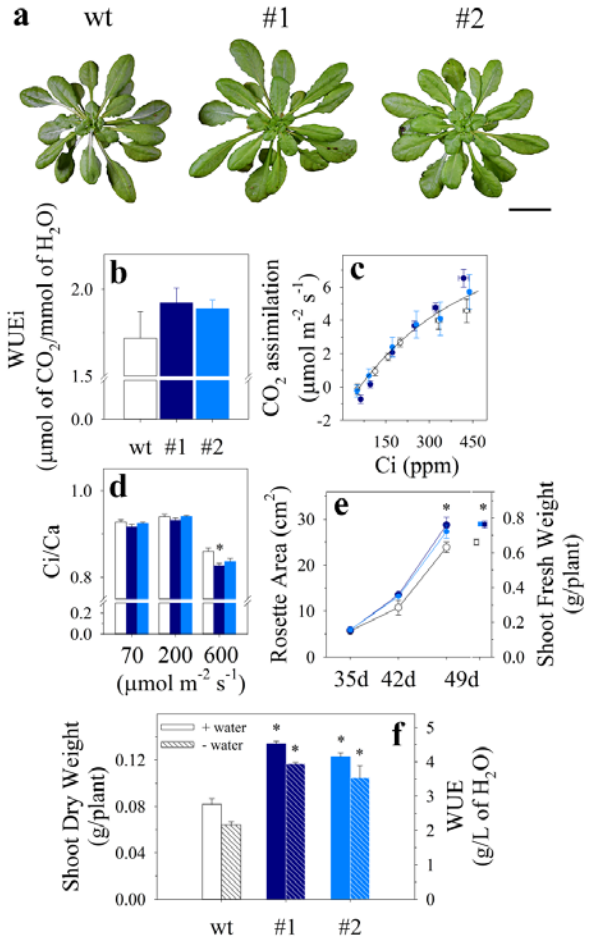

Figure 3. BLINK1 expression enhances photosynthetic carbon assimilation and water use efficiency. Plants were grown under diel cycles with white light fluctuating at 1-h intervals between 10 to 150 µmol m^{-2} s^{-1}, at 390 µL/L CO_2, 22ºC and 55% relative humidity. Scale bar, 5 cm. **(a)** Representative wt (white) and two wt-BLINK plants (cross-referenced below in dark and light blue). **(b)** Instantaneous water use efficiency (WUEi), **(c)** relationship of CO_2 assimilation to intracellular CO_2 concentration (C_i) at saturating (1000 µmol m^{-2} s^{-1}) white light and **(d)** Ci/Ca ratio at 70, 200 and 600 µmol m^{-2} s^{-1} of white light. Data are means ±SE (n=4 for each line). **(e,f)** Long-term plant growth measured as rosette area and shoot fresh weight **(e)** and as shoot dry weight and WUE **(f)** determined for each experiment as dry biomass per liter of water applied. Data in **(f)** is for plants grown under water-replete (+water, open and

358 solid bars) and water-deficit (-water, hatched bars) conditions. Data are means ±SE (n=15
359 water-replete; n=6 water-deficit). Asterisks indicate statistically significant differences
360 compared to wt by student's t-test ($P<0.05$).

361
362
363
364
365
366

367

368

Supplementary Materials for

Optogenetic manipulation of stomatal kinetics improves carbon assimilation and water use efficiency

Papanatsiou, M., Petersen, J., Henderson, L., Wang, Y., Christie, J.M., and Blatt, M.R.
correspondence to: michael.blatt@glasgow.ac.uk

This PDF file includes:

Material and Methods

Plant Material and Growth

Wild-type (wt) Arabidopsis thaliana L. Heynh. (gl-1, ecotype Columbia) and the double mutant *phot1-5 phot2-1* (*p1p2*) were described previously (*9*). Plants were grown in short day conditions (8-h-light/16-h-dark cycle with, 22°C/18°C, and 60% and 70% relative humidity). Three daylight regimes of were used for growth experiments, either with steady 75 or 190 µmol m^{-2} s^{-1} or with light stepped at 1-h intervals at light intensities ranging between 10 and 150 µmol m^{-2} s^{-1}. For growth under water-deficit, after 21 d soil moisture was monitored daily with a Delta-T HH2-ML3 moisture sensor (Delta-T Devices, Cambridge UK) and maintained at 10% with water as required.

Stable Transformation

For stable transformations, the plasmid pEZR(K)-LN (*30*) was digested with SacI and BamHI. The primer pairs CTCACTATAGGGAGCTCACAAGGACACAAGGACATATG

and CATCCCATTAAGCCTGCTTTTTTGTACAAAC were used to amplify the guard-cell promoter (pMYB60) (*13, 31*), and the primer pairs CAGGCTTAATGGGATGTACAGTCTCTGC and CAGCGGCAGCAGCCGTCATAAAGTTAGAACGATGAAG were used to amplify the BLINK1 coding sequence (*11*). The final pEZ pMYB60::BLINK1 construct was generated by Gibson Assembly.

Transformation of *Arabidopsis thaliana gl1* and *phot1-5 phot2-1* (*14*) with Agrobacterium was performed as described previously (*32*). T3 lines with a single transgene locus were selected by segregation of the kanamycin resistance (*33*).

Transient Transformation of *Nicotiana benthamiana* and Arabidopsis

For transient expression of BLINK1 under the control of the CaMV 35S promoter in *N. benthamiana*, the entry clone was generated by PCR using specific primers containing attB3 5'-GGGGACAACTTTGTATAATAAAGTTGTCAACATGGGATGTACAGTCTCTGCAGA G-3' and attB2 sites 5'-GGGGACCACTTTGTACAAGAAAGCTGGGTATCATAAAGTTAGAACGATGAAGAA CACTG-3'. The gel purified PCR product was used together with the pDONR 221 P3-P2 vector to create the final DONR vector using BP-clonase II (Life technologies) according to the manufacturer's instructions. After verifying the product of the BP-reaction by sequencing, LR-clonase II (Life Technologies) was used together with the pFRET cg-2in1-cc vector (*34*) to generate the final destination vector pFRET cg-2in1-cc BLINK1/mCherry. Infiltration of *N. benthamiana* leaves was performed with transformed Agrobacterium as described previously (*35*). Transient transformation of Arabidopsis roots was performed as described previously (*12*).

Immunoblot Analysis

Total protein extracts were prepared from *N. benthamiana* leaf discs 3 days post infiltration. Plant tissue was ground with a pestle in SDS sample buffer (62.5 mM Tris-HCl, pH 6.8, 2% SDS, 10% glycerol, 5% 1mM DTT, 0.004% bromophenol blue) and centrifuged at 10,000 g, at 4 °C for 5 min. Half of the supernatant was directly used for immunoblot analysis of the BLINK1 tetramer (unboiled sample). Protein samples were subjected to 7.5% SDS-PAGE detection for the BLINK1 tetramer. Proteins were transferred onto nitrocellulose membrane (BioRad) by electroblotting and detected with anti-Kcv antibody (*36*). Blots were developed with horseradish peroxidase (HRP)-linked secondary antibodies (Promega) and Pierce ECL Plus Western Blotting Substrate (Thermo Fisher Scientific).

Gas Exchange and Stomatal Apertures

Gas exchange measurements were carried out using the LI-COR 6400 XT Infrared Gas Analyzer (LICOR Biosciences) and whole-plant Arabidopsis chamber (LI-COR 6400-17) (*37*). Light was adjusted using an integrated RGB light source (LI-COR 6400-18). Stomatal conductance was calculated from transpiration rates at a temperature of 22°C. Measurements were carried out over the same period of the diurnal cycle and were normalised to rosette area calculated from images using ImageJ 1.43u (http://rsb.info.nih.gov/ij).

Apertures were recorded from stomata in epidermal peels continuously superfused with 5 mM Ca^{2+}-MES, pH 6.1, with 10 mM KCl(*33, 37*), in the dark and under RL and/or BL of 100 µmol m^{-2} s^{-1} for 2 h. Following measurements, the stomata were incubated for 5 min in buffer supplemented with 20 µM fluorescein diacetate to confirm viability. Only stomata with guard cells retaining a fluorescein signal under confocal fluorescence microscopy were included for analysis.

RNA Extraction and Real-Time PCR

Total RNA was extracted from leaf tissue from 4-week old plants using Plant RNeasy Mini kit, and cDNA synthesis was carried out using Quanti-script (Qiagen) kit. Real-time PCR was carried out using Brilliant III Ultra-Fast SYBR QPCR kit (Applied Biosystems) with primer pairs ATGGAACTGAGCATGTCCGA and TTTTGTCCGGGTTTGCAACA to amplify *BLINK*, and GCCATCGCTTCTTCATCTGTTGC and GTGGGGAGAGAAAGATGCTTTGCG to amplify the reference *ISU* gene (*29*). For each transcript, amplification was assayed over a range of cycle numbers to select optimal conditions for visualization of the PCR product and quantification.

Guard Cell Electrophysiology

Voltages and current clamp data were recorded from Arabidopsis root epidermal cells and intact guard cells in epidermal peels using Henry's EP Software Suite (http://www.psrg.org.uk). Double-barrelled microelectrodes (tip resistances >100 MΩ) were filled with 200 mM K^+-acetate (pH 7.5) as described previously (*37-40*) after equilibration

opening, the mean K^+ flux needed to drive opening is 10 amol s^{-1}, equivalent to a current of 0.9 pA. This value is below the limit of resolution for whole-cell voltage clamp measurements from plant cells. It represents less than 0.5% of the K^+ currents typically recorded when Arabidopsis guard cells are clamped near the voltage extremes more than ±100 mV from the free-running voltage (*5*).

Total Protein and Total Starch Quantification

Leaves were harvested into liquid nitrogen and finely ground. 20 mg of material was weighed to extract total starch using Starch GO/B Assay kit (Sigma, Poole UK) according to the manufacturer's instructions. 10 mg of material was weighed to extract protein using homogenization buffer [0.0625M Tris·HCl pH 6.8, 1% (wt/vol) SDS,10% (vol/vol) glycerol, and 0.01% (vol/vol) 2-mercaptoethanol]. Samples were incubated at 65 °C for 10 min before centrifuging at 13000 rpm for 10 min. Supernatant was collected and protein was quantified using Pierce BCA kit (Thermo Scientific, Loughborough, UK) according to the manufacturer's instructions.

Statistical Analysis

Statistically significance was determined by Student's t-test or ANOVA at $P< 0.05$ using SigmaPlot12 (Systat) software. Data are reported as means ±SE of n observations with the exception of stomatal assays which are reported as medians ±SE along with 0.25 – 0.75 ranges.

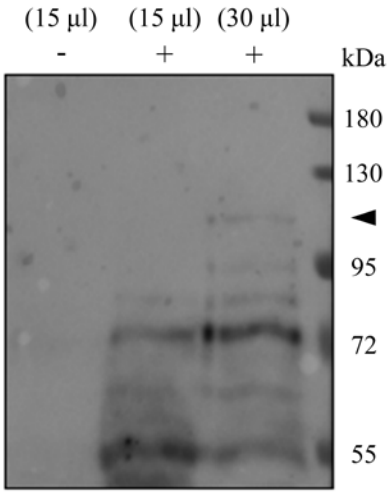

Fig. S1. Functional tetramer formation of BLINK1 *in planta*. Immunoblot analysis of total protein extracts from *N. benthamiana* leaves BLINK1 (+) or not expressing BLINK1 (-). The protein extract volumes indicated were probed with anti-Kcv monoclonal antibody recognizing specifically the tetrameric form of the channel. Expected Mw of BLINK1 is 106.5 kDa. Lower Mw bands likely represent proteolytic cleavage products. Black arrow indicates the tetramer formation of BLINK1.

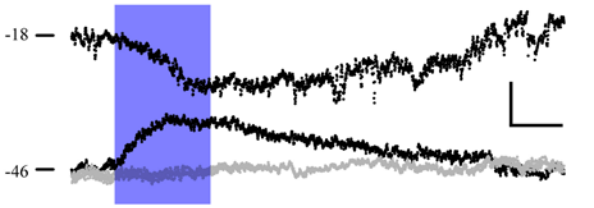

Fig. S2. BLINK1 photoactivation drives the membrane towards the K^+ equilibrium voltage (E_K). Representative recordings of membrane voltage in 5 mM Ca^{2+}-MES, pH 6.1, with 30 mM KCl from wt (grey) and transiently BLINK1-transformed (black) Arabidopsis roots(*12*). Treatments with 100 µmol m^{-2} s^{-1} BL indicated by shading. Scale bar: 10 mV, vertical; 2 min, horizontal. Estimated E_K, -30 mV. Mean halftimes and voltage displacements: 89±8 s (+BL); 351±24 s (-BL); 15±2 mV (n=10).

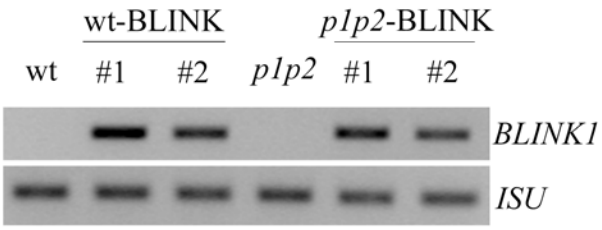

Fig. S3. *BLINK1* expression in Arabidopsis plants. RT-PCR analysis of *BLINK1* expression compared to reference gene *ISU* (*29*) from wild-type, *p1p2* double mutant, wt-BLINK and *p1p2*-BLINK transgenic plants.

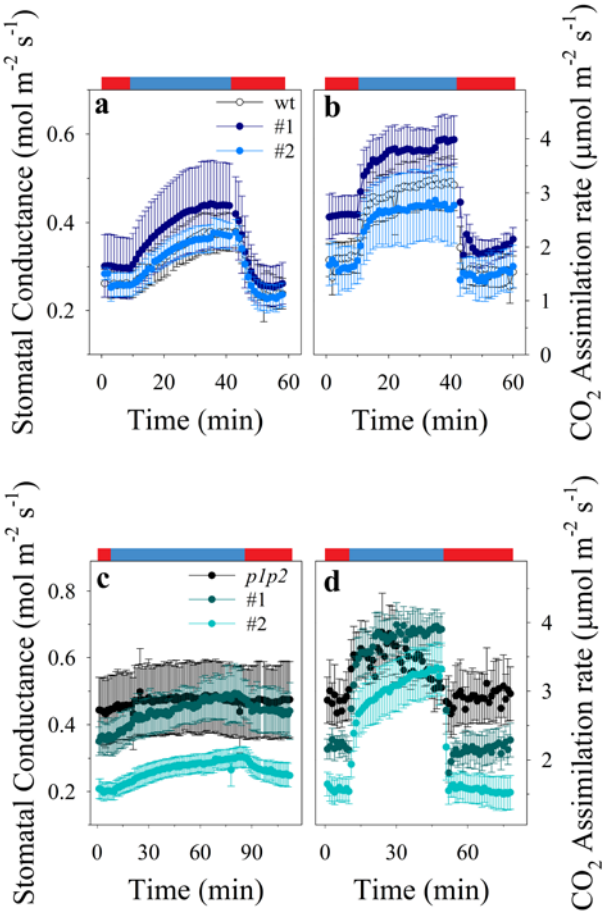

Fig. S4. BLINK1 photoactivation stimulates stomatal opening. Stomatal conductance **(a, c)** and CO_2 assimilation rates **(b, d)** measured from RL-adapted wt, wt-BLINK, *p1p2* and *p1p2*-BLINK plants on adding 100 µmol m^{-2} s^{-1} BL. Transitions from RL to RL+BL were carried out once stomatal conductances reached a steady state. Data are means ±SE (n=5 for each line).

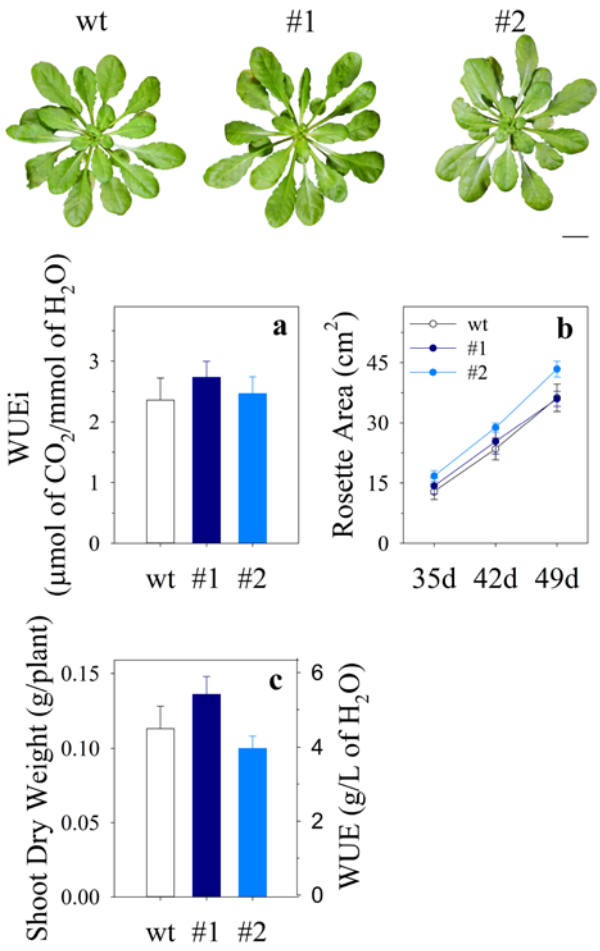

Fig. S5. BLINK1 has a marginal effect on carbon assimilation and WUE under diel cycles of continuous low light intensity. Wild type (white) and two wt-BLINK transgenic plants (dark and light blue bars and symbols) were grown under diel cycles of with steady illumination of 75 µmol m^{-2} s^{-1}. Scale bar, 5 cm (*above*). **(a)** WUEi calculated from plants exposed to 75 µmol m^{-2} s^{-1} of homogeneous white light, at 390 ppm of CO_2, 22ºC and 55% relative humidity. Data are means ±SE (n=4 for each line). **(b,c)** Growth of plants followed for 49 days to measure rosette expansion **(b)** and accumulation of dry biomass and long term WUE **(c)**. Data are means ±SE (n=10 independent experiments).

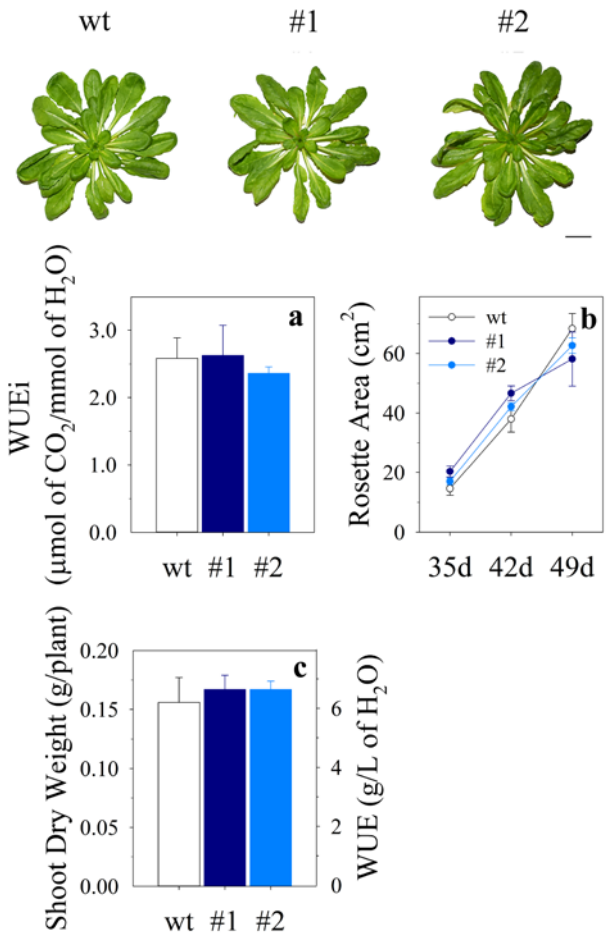

Fig. S6. BLINK1 has a marginal effect on carbon assimilation and WUE under diel cycles of continuous high light intensity. Wild type (white) and two wt-BLINK transgenic plants (dark and light blue bars and symbols) were grown under diel cycles of with steady illumination of 190 µmol m^{-2} s^{-1}. Scale bar, 10 cm (*above*). **(a)** WUEi calculated from plants exposed to 190 µmol m^{-2} s^{-1} of homogeneous white light, at 390 ppm of CO_2, 22ºC and 55% relative humidity. Data are means ±SE (n=4 for each line). **(b,c)** Growth of plants followed for 49 days to measure rosette expansion **(b)** and accumulation of dry biomass and long term WUE **(c)**. Data are means ±SE (n=10 independent experiments).

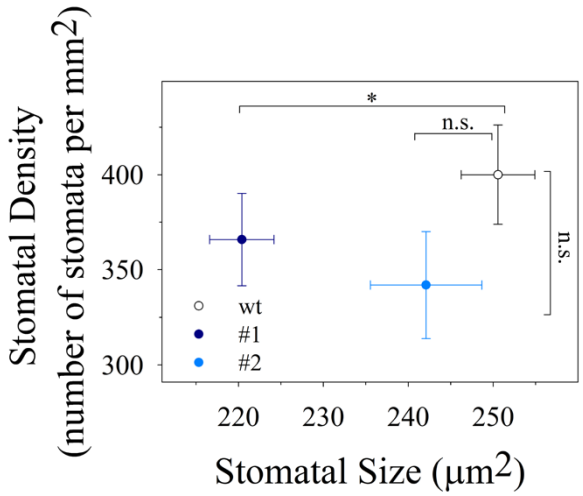

Fig. S7. BLINK1 expression did not alter stomatal characteristics. Stomatal density and size (area of the stomatal complex) were measured from epidermal peels subjected to blue light treatment. Data are means ±SE (n=40 stomata). Asterisk indicates statistically significant difference by student's t-test ($P<0.05$).

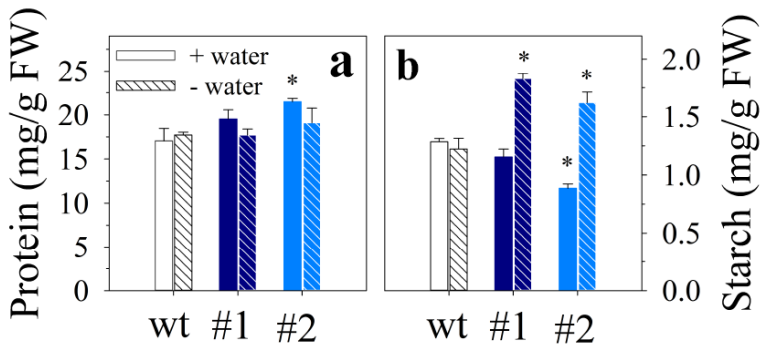

Fig. S8. BLINK1 induces starch accumulation under water limited conditions. Plants were grown under diel cycles with white light fluctuating at 1-h intervals between 10 to 150 µmol m^{-2} s^{-1}, at 390 µL/L CO_2, 22ºC and 55% relative humidity. Plants exposed to two water regimes, water-replete (+water; open and solid bars) and water-deficit (-water; hatched bars) with 10% soil moisture. **a)** Total protein amount and **(b)** total starch amount, quantified as mg per g of fresh shoot weight. Data are means ±SE (n=4). Asterisks indicate statistically significant differences, determined by student's t-test ($P<0.05$).

Table S1. Gas exchange characteristics of BLINK1 transgenic and wild type plants adapted to either darkness or red light.

		Blue light ON		Blue light OFF	
		Max. Stomatal Conductance (mol m^{-2} s^{-1})	Opening Halftime (min)	Min. Stomatal Conductance (mol m^{-2} s^{-1})	Closing Halftime (min)
Dark - Blue Light Response	wt	0.49 ±0.03	40.32 ±2.65	0.28 ±0.05	4.94 ±0.48
	#1	0.50 ±0.03	22.94 ±0.34 *(P<0.001)*	0.22 ±0.03	3.64 ±0.34 *(P=0.03)*
	#2	0.59 ±0.04	23.90 ±6.09 *(P=0.045)*	0.22 ±0.03	3.18 ±0.47 *(P=0.019)*
Red - Blue Light Response	wt	0.46 ±0.05	24.46 ±7.39	0.22 ±0.03	4.41 ±0.77
	#1	0.50 ±0.09	6.69 ±1.06 *(P=0.012)*	0.20 ±0.04	1.81 ±0.48 *(P=0.013)*
	#2	0.38 ±0.04	6.37 ±1.23 *(P=0.007)*	0.20 ±0.03	2.98 ±0.39 *(P=0.045)*

Table S2. Growth characteristics of BLINK1-transgenic, wild type and *p1p2* plants grown under two continuous light regimes.

			wt-BLINK			*p1p2*-BLINK	
		wt	**#1**	**#2**	***p1p2***	**#1**	**#2**
LWL (75 µmol m^{-2} s^{-1})	Fresh Weight (g)	0.94 ±0.09	1.21 ±0.17	1.12 ±0.09	0.41 ±0.05	0.39 ±0.08	0.44 ±0.05
	Dry Weight (g)	0.11 ±0.02	0.14 ±0.01	0.10 ±0.02	0.04 ±0.005	0.05 ±0.01	0.04 ±0.01
	Rosette Area (cm^2)	36.26 ±3.40	36.00 ±1.87	43.85 ±1.95	13.67 ±2.22	9.72 ±0.90	13.83 ±1.75
	WUEi (µmol of CO_2/mmol of H_2O)	2.36 ±0.36	2.73 ±0.36	2.47 ±0.27	-	-	-
	WUE (g/L of H_2O)	4.52 ±0.60	5.43 ±0.48	4.00 ±0.32	1.46 ±0.22	1.81 ±0.43	1.72 ±0.33
	FW:DW	8.56 ±0.18	8.64 ±0.16	11.2 ±0.13 *(P<0.001)*	10.25 ±0.02	7.80 ±0.04	11.00 ±0.06
HWL (200 µmol m^{-2} s^{-1})	Fresh Weight (g)	2.00 ±0.25	2.07 ±0.21	2.16 ±0.14	1.00 ±0.07	0.72 ±0.14	0.76 ±0.13
	Dry Weight (g)	0.16 ±0.02	0.17± 0.01	0.17 ±0.007	0.08 ±0.02	0.06 ±0.01	0.05 ±0.02
	Rosette Area (cm^2)	68.31 ±5.09	58.11 ±9.08	62.62 ±2.62	24.26 ±1.15	21.27 ±3.60	19.60 ±2.18
	WUEi (µmol of CO_2/mmol of H_2O)	2.58 ±0.30	2.62 ±0.45	2.36 ±0.10	-	-	-
	WUE (g/L of H_2O)	6.23 ±0.84	6.66 ±0.46	6.69 ±0.29	3.29 ±0.80	2.07 ±0.53	1.85 ±0.30
	FW:DW	12.5 ±0.016	12.18 ±0.01	12.71 ±0.004	12.5 ±0.06	12.00 ±0.03	15.2 ±0.16

Table S3. Growth characteristics of BLINK1-transgenic, wild type and *p1p2* plants grown under fluctuating light and two water regimes.

			wt-BLINK			*p1p2*-BLINK	
		wt	**#1**	**#2**	***p1p2***	**#1**	**#2**
Fluctuating white light (water-sufficient)	Fresh Weight (g)	0.66 ±0.02	0.77 ±0.07 *(P<0.001)*	0.72 ±0.06 *(P=0.001)*	0.34 ±0.01	0.45 ±0.05	0.39 ±0.05
	Dry Weight (g)	0.082 ±0.005	0.13 ±0.002 *(P<0.001)*	0.12 ±0.003 *(P<0.001)*	0.05 ±0.01	0.09 ±0.03	0.07 ±0.02
	Rosette Area (cm^2)	23.87 ±1.13	28.72 ±1.67 *(P=0.027)*	27.28 ±1.45 *(P=0.048)*	11.06 ±0.72	13.77 ±0.73	12.83 ±0.96
	WUEi (µmol of CO_2/mmol of H_2O)	1.72 ±0.15	1.92 ±0.08	1.89 ±0.05	-	-	-
	WUE (g/L of H_2O)	2.67 ±0.16	4.19 ±0.08 *(P<0.001)*	4.15 ±0.10 *(P<0.001)*	2.18 ±0.57	2.78 ±0.79	2.84 ±0.78
	FW:DW	8.054 ±0.001	5.926 ±0.008 *(P<0.001)*	6.006 ±0.007 *(P<0.001)*	6.80 ±0.04	5.00 ±0.11	5.57 ±0.08
Fluctuating white light (water-limited)	Fresh Weight (g)	0.60 ±0.005	0.75 ±0.09	0.71 ±0.003	-	-	-
	Dry Weight (g)	0.064 ±0.003	0.121 ±0.001 *(P<0.001)*	0.11 ±0.01 *(P=0.003)*	-	-	-
	Rosette Area (cm^2)	26.78 ±1.18	26.18 ±0.69	28.07 ±1.01	-	-	-
	WUE (g/L of H_2O)	2.08 ±0.11	3.66 ±0.03 *(P<0.001)*	3.52 ±0.32 *(P=0.008)*	-	-	-
	FW:DW	9.46 ±0.08	6.47 ±0.09 *(P<0.001)*	6.81 ±0.03 *(P<0.001)*	-	-	-